

# Biobased poly(3-hydroxybutyrate acid) composites with addition of aliphatic polyurethane based on polypropylene glycols

IWONA ZARZYKA<sup>1\*</sup>, ANNA CZERNIECKA-KUBICKA<sup>2,3</sup>, KAROL HĘCLI<sup>1</sup>, LUCJAN DOBROWOLSKI<sup>1</sup>,  
BEATA KRZYKOWSKA<sup>1</sup>, ANITA BIAŁKOWSKA<sup>4</sup>, MOHAMED BAKAR<sup>4</sup>

<sup>1</sup> Faculty of Chemistry, Rzeszow University of Technology, Rzeszów, Poland.

<sup>2</sup> Department of Experimental and Clinical Pharmacology, Medical College of Rzeszów University,  
The University of Rzeszów, Rzeszów, Poland.

<sup>3</sup> Interdisciplinary Center Preclinical and Clinical Research, The University of Rzeszów, Rzeszów, Poland.

<sup>4</sup> Faculty of Chemical Engineering and Commodity Science, University of Technology and Humanities, Radom, Poland.

Poly(3-hydroxybutyrate) (P3HB) is the most important of the polyhydroxyalkanoates. It is biosynthesized, biodegradable, biocompatible, and shows no cytotoxicity and mutagenicity. P3HB is a natural metabolite in the human body and, therefore, it could replace the synthetic, hard-to-degrade polymers used in the production of implants. However, P3HB is a brittle material with limited thermal stability. Therefore, in order to improve its mechanical properties and processing parameters by separating its melting point and degradation temperature, P3HB-based composites can be produced using, for example, linear aliphatic polyurethanes as modifiers. The aim of the study is a modification of P3HB properties with the use of linear aliphatic polyurethanes synthesized in reaction of hexamethylene diisocyanate (HDI) and polypropylene glycols (PPG) by producing their composites.

Prepared biocomposites were tested by the scanning electron microscopy (SEM), differential scanning calorimetry (DSC) and thermogravimetry (TGA). Furthermore, selected mechanical properties were evaluated. It has been confirmed that new biocomposites showed an increase in impact strength, relative strain at break, decrease of hardness and higher degradation temperature compared to the unfilled P3HB. The biocomposites also showed a decrease in the glass transition temperature and the degree of crystallinity. Biocomposites obtained with 10 wt.% polyurethane synthesized with polypropylene glycol having  $1000 \text{ g} \cdot \text{mole}^{-1}$  and HDI have the best thermal and mechanical properties.

*Key words: P3HB composites, polyurethanes, hexamethylene diisocyanate, polypropylene glycol, thermal and mechanical properties, morphology*

## 1. Introduction

Because of growing environmental pollution, biodegradable materials, materials of natural origin and biopolymers have significant importance [4], [8], [10], [14], [18], [20], [21]. Natural biopolymers, such as paper and silk have been used for a long time. Biocomposites of natural origin have also been used since antiquity, e.g., clay bricks with the addition of straw

[15]. Unfortunately, in the 20th century, natural polymers were almost replaced by the cheap petroleum-based synthetic polymers. Growing environmental pollution has sparked the renewed interest in biopolymers because they are environmentally friendly. Biopolymers have a great advantage over conventional polymers due to their sourcing from renewable sources and easy and quick degradation. It is extremely important especially in the production of items with a short service life [9].

---

\* Corresponding author: Iwona Zarzyka, Faculty of Chemistry, Rzeszow University of Technology, ul. Powstańców Warszawy 6, 35-959 Rzeszów, Poland. Phone: +480178651762, fax.: +480178543655, e-mail: izarzyka@prz.edu.pl

Received: November 19th, 2021

Accepted for publication: January 14th, 2022

Polyhydroxyalkanoates have a particular importance among the biopolymers because they are bio-synthesized and biodegradable. Poly(3-hydroxybutyrate) (P3HB) is the most important polyhydroxy-alkanoate. It is synthesized and stored by *Ralstonia eutropha* bacteria. Its properties are comparable to those of isotactic polypropylene. An additional advantage of P3HB is its biocompatibility and the lack of cytotoxicity and mutagenicity. In addition, P3HB is a natural metabolite in the human body. Therefore, P3HB could replace synthetic, hard-to-degrade polymers used in medicine as implant for tissue engineering [1], [12], [13], [19]. P3HB and its biocomposites can be also applied to reconstructive therapy for animals and human.

However, P3HB is a brittle material with a limited thermal stability. In order to improve its mechanical properties and processing parameters, biocomposites can be produced on the P3HB matrix. This should lead to the separation of its melting point and its degradation temperature.

The essence of the work is the production of P3HB biocomposites with the use of linear aliphatic polyurethanes obtained by the reaction of hexamethylene diisocyanate and polypropylene glycols with a molecular weight of 400 and 1000 g·mole<sup>-1</sup>. Obtained biocomposites should be characterized by better thermal and mechanical properties than the unfilled P3HB.

## 2. Materials and methods

### 2.1. Materials

P3HB was purchased from Biomer (Germany). The rest of reagents: hexamethylene diisocyanate (HDI), polypropylene glycols with molecular weight 400 g·mole<sup>-1</sup> (PPG400) and 1000 g·mole<sup>-1</sup> (PPG1000), dibutyltin dilaurate (DBTL) and acetone were supplied by Aldrich (Germany).

### 2.2. Preparation of linear polyurethanes

Prior to synthesis, the polypropylene glycols (PPG) were dried with toluene in an azeotropic water removal process. After distillation, toluene was removed under reduced pressure. Finally, the hydroxyl number of the dried glycol was determined according to PN-92/C-8905203.

The dried PPG400 dissolved in anhydrous acetone and DBTL were placed in a three-necked round-bottomed flask equipped with a mechanical stirrer, dropping funnel and thermometer. HDI was added dropwise to the solution in such an amount that the ratio of the molar ratio of isocyanate to hydroxyl groups of the glycol was 1 : 1.08. The temperature of the mixture was kept below 20 °C by controlling of the rate of the dropwise addition. The reaction was carried out under nitrogen atmosphere for about 6 hours until the exothermic effect disappeared. The end of the synthesis was determined on the basis of the increase in the viscosity of the reaction mixture and the value of the determined isocyanate number according to PN-EN 1242.2006. When the reaction was completed, acetone was removed. The constant weight of the final product (PU400) was obtained after an exposure in a vacuum oven in the temperature range of 40–100 °C. The synthesis of polyurethane with PPG1000 (PU1000) was carried out analogously.

### 2.3. Biocomposites preparation

Biocomposites based on P3HB were obtained with the use of 5, 10, 15 and 20 wt.% PU400 and PU1000. The biocomposite designation is given in Table 1. First, P3HB was dried for 30 minutes at temperature 40 °C under reduced pressure. Next, P3HB and the appropriate amount of polyurethane were mixed for 20 minutes at room temperature in a tumble mixer. Then, the homogenized mixture was introduced into a co-rotating twin-screw extruder ZE-25-33D by Berstorff and the polymer biocomposite was extruded at 320 rpm in the temperature range of 120–170 °C. The molten product exited the extruder through the twin strand head. After cooling in a cooling bath, the biocomposite was granulated and dried at 60 °C for more than 2 hours. Due to technical problems, it was not possible to extrude a polymer mixture containing 20 wt. % of PU-1000.

Table 1. Designation of the produced P3HB biocomposites

Type of glycol in PU	PU concentration in biocomposite (wt. %)	Biocomposite designation
PPG400	5	PU400-5
PPG400	10	PU400-10
PPG400	15	PU400-15
PPG400	20	PU400-20
PPG1000	5	PU1000-5
PPG1000	10	PU1000-10
PPG1000	15	PU1000-15

## 2.4. Analytical methods

### 2.4.1. Size exclusion chromatography of linear polyurethanes

The measurement of the molar weight of polyurethanes was carried out by means of size exclusion chromatography (SEC) using the following apparatus and measurement conditions: Viscotek degasser, columns (PSS SDV Guard and PSS SDV 100 Å, 1000 Å, grain diameter 5 µm), Shimadzu LC-20AD isocratic pump, Shodex RI-71 differential refractometer, solvent: tetrahydrofuran (THF), THF flow rate: 1 ml · min<sup>-1</sup>, temperature: 22 °C, loop volume: 100 µl, OmniSEC software version 4.2.

Prior to making the measurements, the chromatographic system was calibrated with polystyrene patterns. Number-average ( $\overline{M}_n$ ) and weight-average ( $\overline{M}_w$ ) molar weights and dispersity ( $D = \overline{M}_w \cdot \overline{M}_n^{-1}$ ) of the polyurethanes (PU400 and PU1000) are given in Table 2.

### 2.4.2. FTIR spectra

The FTIR spectrum of P3HB in the form of a KBr pellet, and the spectra of polyurethanes and composites were made using the ATR technique with the use of the ALPHA FT-IR apparatus from BRUKER. The spectra were measured with a resolution of 0.01 cm<sup>-1</sup> in the range 4000–500 cm<sup>-1</sup>.

### 2.4.3. Scanning electron microscope measurements

The produced composites on the P3HB matrix and the unfilled P3HB were tested using a scanning electron microscope with an X-ray energy dispersion analyzer for chemical analysis in the micro-area. First, the samples were frozen in liquid nitrogen and then broken under impact. The fracture surfaces of biocomposites were analyzed. The broken samples were covered with a layer of gold with a thickness of approx. 10 nm using a gold sputtering machine. Finally, photomicrographs were obtained showing the structure and morphology of the composite surfaces.

### 2.4.4. TG measurements

The thermogravimetric analysis of P3HB and their biocomposites was performed using a Metler Toledo TGA / SDTA 851e thermogravimetric analyzer. The samples were heated at a rate of 10 and 5 °C · min<sup>-1</sup> in the temperature range from +25 to +600 °C under

nitrogen atmosphere. The decomposition onset temperature ( $T_{on}$ ), the 50% weight loss temperature ( $T_{50\%}$ ), the maximum decomposition rate temperature ( $T_{max}$ ) and the total weight loss of the sample at 600 °C were determined.

### 2.4.5. Digital scanning calorimetry measurements

The DSC measurements of P3HB and its biocomposites were carried out using a differential scanning calorimeter (TA Instrument Q25), obtaining results in the form of a heat flow dependence on temperature or time as a response to a linear change of temperature with time. All analyses were performed under a nitrogen atmosphere which was kept constant at about 50 ml · min<sup>-1</sup>. Calibration of temperature and heat flow in calorimeters was carried out in relation to the melting parameters of indium, i.e., the initial melting point, the so-called “Onset”:  $T_m(\text{onset}) = 156.6$  °C (429.6 K) and enthalpy of fusion  $\Delta H_f = 28.45$  J · g<sup>-1</sup> (3.28 kJ · mol<sup>-1</sup>).

The weights of the prepared, tested samples ranged from 5 to 10 mg. The accuracy of measurements was ±3%. Standard Differential Scanning Calorimetry measurements were carried out over a temperature range of -40 to 195 °C, with a variable cooling rate in the range of 1–40 °C · min<sup>-1</sup> and a constant heating rate of 10 °C · min<sup>-1</sup>. An isothermal annealing was performed for 2 minutes at 195 °C and the system was stabilized for 5 minutes at -40 °C.

### 2.4.6. Selected mechanical properties

The specimens for mechanical tests were obtained by injection method using an injection moulding machine. The process was carried out in the temperature range of 140–169 °C, the temperature of the injection mould was 25 °C for the unfilled P3HB and 30 °C for composites; the pressure of 250–280 bar for composites and 550 bar for P3HB. The specimens were produced in accordance with the standard PN EN ISO 527 (1998). The selected mechanical properties of the prepared biocomposites were evaluated and compared to those of the unfilled P3HB. Tensile strength, elongation at break, Brinell hardness and Charpy impact strength were determined. The tensile mechanical properties were determined according to the standard PN-EN ISO 527-2: 2012.05. Tensile strength and elongation at break measurements were performed under the condition of a jaw feed rate of 5 mm · min<sup>-1</sup>. Charpy impact strength tests were performed according to the standard PN-EN ISO 179-1: 2010 using a Zwick 5102

apparatus. Hardness was determined by the Brinell method in accordance with the standard PN-EN ISO 6506-1: 2014 using the Zwick apparatus.

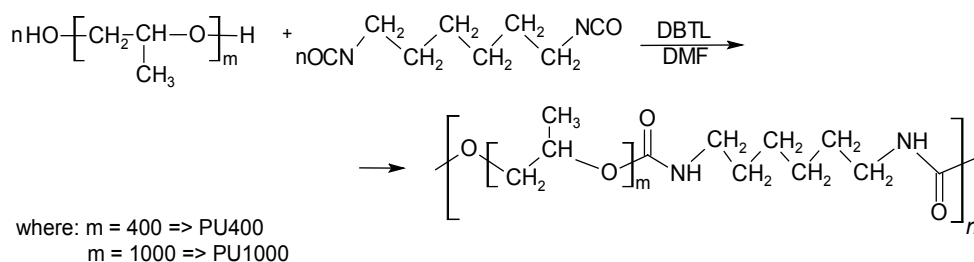
## 2.5. Statistical analysis

Statistical calculations were performed with the *Statistica* software (version 13). A separate datasheet has been created for each mechanical property. Statistical tests were performed for each of the mechanical properties of the obtained samples. The data were verified prior to testing. Therefore, a normality plot was created for each variable to check for outliers in the data. Such values were removed from the data sheet. Moreover, The Shapiro–Wilk test was used to check whether the variables were normally distributed. Then the *t*-test (Student test) was performed. The *t*-test is a statistical method for comparing two means with each other.

## 3. Results

### 3.1. Synthesis and characterization of linear aliphatic polyurethanes

Aliphatic linear polyurethanes obtained by reacting polypropylene glycols such as PPG400 and PPG1000 with HDI were used to improve the properties of P3HB:



The molar weights of polyurethanes obtained with the use of PPG400 (PU400) were twice as large as the molar weights of PUs synthesized in the reaction with PPG1000 (PU1000). Similarly, their dispersity was slightly higher, reaching 2.09 and 1.62, respectively for PU400 and PU1000, as shown in Table 2.

Table 2. Molar weights and dispersity of resulted polyurethanes PU400 and PU1000

PU	$M_n$ [g · mole <sup>-1</sup> ]	$M_w$ [g · mole <sup>-1</sup> ]	$D = M_w \cdot M_n^{-1}$
PU400	22360	26850	2.09
PU1000	11180	18170	1.62

### 3.2. P3HB-based biocomposites preparation

The prepared polyurethanes PU400 and PU1000 were used to modify the properties of P3HB. We used 5, 10, 15 and 20 wt.% of PU400 and PU1000. The prepared blends were mixed in the melt state using a twin-screw extruder to obtain biocomposites based on P3HB.

### 3.3. Morphology characterization of the biocomposites

SEM Micrographs were taken showing the surface morphology of P3HB biocomposites containing 5, 10, 15 and 20 wt. % of PU400 and PU1000. For comparison, a micrograph of the extruded unfilled P3HB sample was also performed. The images were obtained by scanning of the fracture surfaces of the prepared samples. SEM micrographs of the fracture surfaces of P3HB and its biocomposites containing PU400 and PU1000 are presented in Figs. 1, 2 and 3. The fracture surface of the unmodified P3HB sample shows a slightly wavy and glassy morphology (Fig. 1), which indicated the presence of a regular and elastic crack propagation path.

In Figure 2, the breakthrough of P3HB based composites modified with an increasing amount of a poly-

urethane modifier based on short-chain PPG400. The polyester contained 5, 10, 15 and 20 wt. % of PU400, respectively.

The biocomposite samples containing polyurethane modifier were characterized by the presence of wavy and rough structures. Such a surface could be seen primarily in the PU400-5 composite containing the smallest (5 wt. %) amount of the modifier based on PPG400. Additionally, uniformly distributed domains with elongated structure were also observed. However, the incorporation of 10 wt. % or 15 wt. % of PU400 (PU400-10 and PU400-15, Fig. 2) into the composite unexpectedly resulted in the disappearance



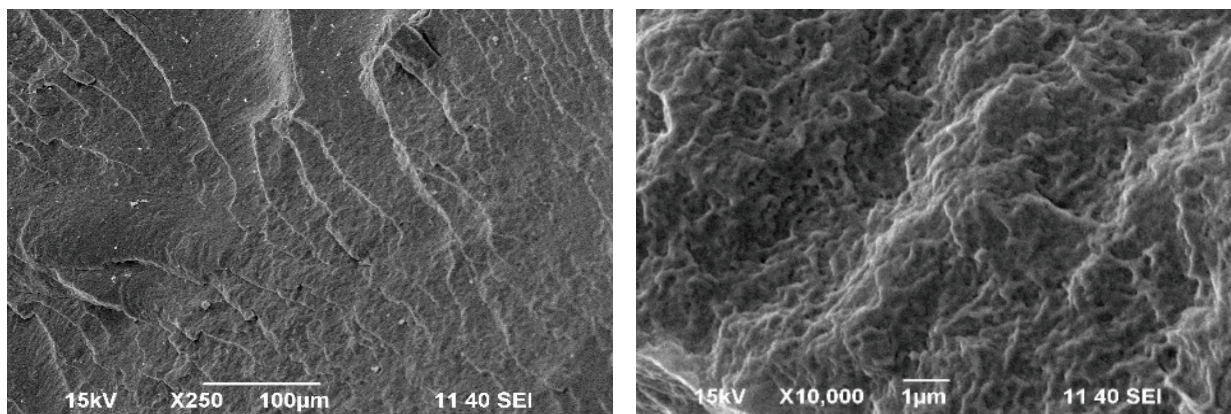


Fig. 1. SEM micrographs of unmodified P3HB with a magnification of 250× and 10000×

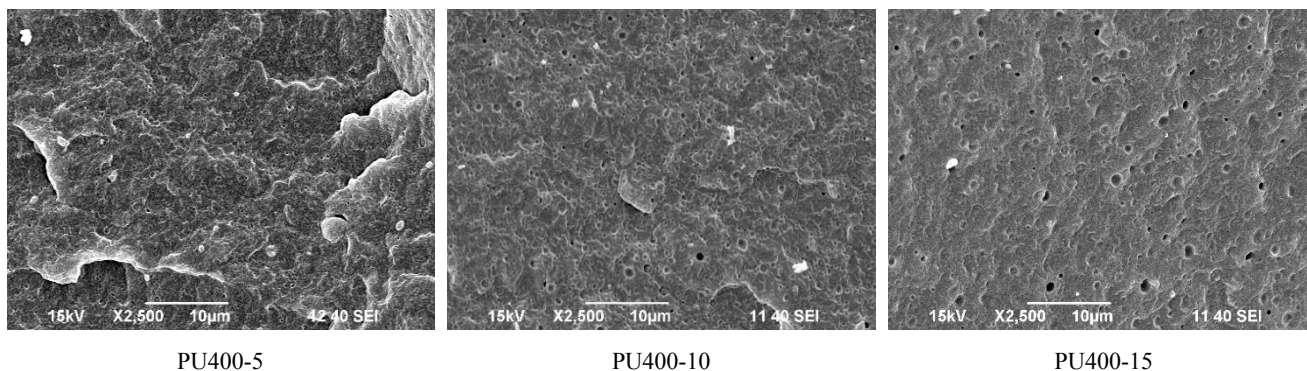


Fig. 2. SEM micrographs of biocomposites of the P3HB matrix containing: 5, 10, and 15 wt. % of PU400 (PU400-5, PU400-10, PU400-15, respectively)

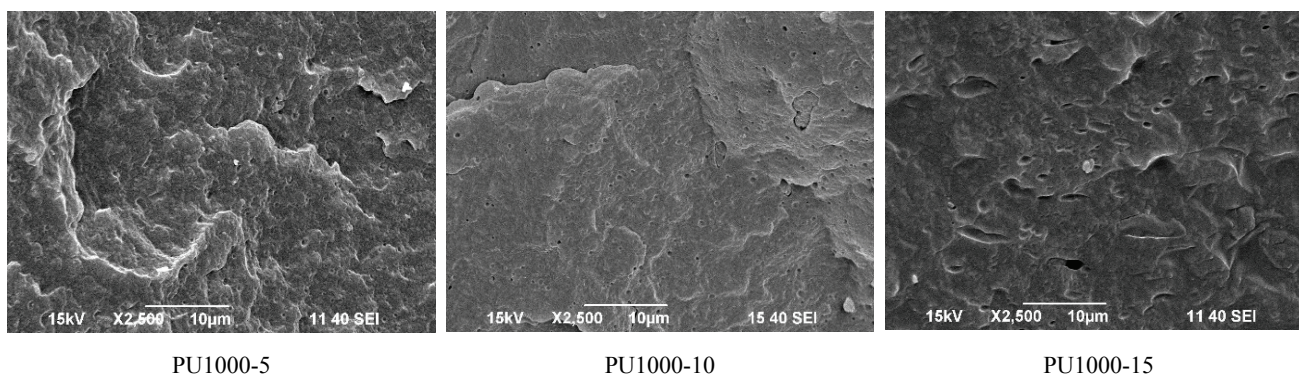


Fig. 3. SEM micrographs of biocomposites on the P3HB matrix containing: 5.0; 10.0; 15.0 and 17.5 wt. % of PU1000 (PU1000-5, PU1000-10, PU1000-15, PU1000-17.5, respectively)

of rough corrugated structures. They appeared again in a composite with 20 wt. % of PU400 (PU400-20). However, unlike in the case of the composite PU400-5, the micrograph of the fracture surface of the composite enriched with the highest amount of PU (PU400-20) shown unevenly distributed rough features.

The micrographs presented in Fig. 3 show the fracture surfaces after crack test of polyester-polyurethane composites containing, 5, 10 and 15 wt. % of PU. The polyurethane modifier used was based on a longer-chain

polypropylene glycol with a higher molecular weight than previously used ( $1000 \text{ g} \cdot \text{mole}^{-1}$ ). The micrographs appear to be different from those of composites based on polyurethane synthesized with PPG400. Compared to the micrograph of the reference sample – the unfilled P3HB, the fracture surfaces of the PPG1000-based PU composites were characterized by the presence of elongated wavy, rough and stratified domains. Composites with 5 wt. % of PU1000 contained an inhomogeneously distributed domains and

wavy rough domains, which could indicate an incompatibility between the components in the blend. However, in composites containing 10 wt. %, and 15 wt. % of PU1000, uniformly distributed domains and rough, wavy areas were noticeable.

The absence of undesirable aggregates in these compositions and the uniform distribution of the domains resulted from the proper homogenization of the polymers used. In these samples (PU1000-10 and PU1000-15), the presence of preferably uniformly distributed elongated domains with rough, wavy areas in the entire sample volume was noticeable. Hence, the addition of 10–15 wt. % of the modifier seemed to be optimal.

### 3.4. Thermal stability of the resulted biocomposites

The thermal stability of the produced biocomposites was tested using the thermogravimetric method, and the interpretation of the results are included in Tables 3 and 4.

Table 3. TG and DTG curves of biocomposites based on P3HB matrix with PU400 and PU1000 addition. The results were obtained at the heating rate of 10 deg · min<sup>-1</sup>

Samples	$T_{on}$ [°C]	$T_{50\%}$ [°C]	$T_{max1}$ [°C]	$T_{max2}$ [°C]	$\Delta m$ [%]
P3HB	271	283	287	–	99.38
PU400	273	339	340	–	97.41
PU400-5	246	248	248	–	98.07
PU400-10	280	288	290	–	99.67
PU400-15	279	288	289	–	99.39
PU400-20	278	288	288	313	99.53
PU1000	281	349	320	422	97.68
PU1000-5	281	290	291	374	99.59
PU1000-10	280	291	291	382	99.50
PU1000-15	281	291	291	382	99.65

The thermal properties of P3HB biocomposites with the addition of PU400 and PU1000 in amount of 5, 10, 15 and 20 wt.% are shown in Table 3. The presence of PU400 and PU1000 made the increase in  $T_{on}$ ,  $T_{50\%}$  and  $T_{max}$  by 7–10, 5–8 and 1–4 °C, respectively. Addition of 20 wt.% of PU400 caused the appearance of a second temperature of the maximum decomposition rate ( $T_{max2}$ ) at 313 °C, which could indicate the composite heterogeneity or migration of the plasticizer. The first one was not confirmed by SEM tests. Moreover, the composite PU400-5 was heterogeneous and had only one the maximum decomposition rate on its DTG curve. TGA curve of PU400 showed only one maximum decomposition rate at temperature 340 °C.

Therefore, it is the evidence of the modifier migration.

$T_{max2}$  occurred also in the case of biocomposites containing PU1000. In this case, it was caused by the presence of a first and second temperatures of the maximum decomposition rate ( $T_{max2}$ ) on DTG curve of PU1000 (Table 3) at 320 and 422 °C, respectively.

Biocomposites with the highest thermal stability, i.e., containing 10 or 15 wt. % of PU400 and PU1000 were tested by thermogravimetric analysis which was performed at a heating rate of 5 °C · min<sup>-1</sup>. In this case, a significant increase in  $T_{on}$ ,  $T_{50\%}$  and  $T_{max}$  was observed by 27–34, 34–39 and 33–38 °C, respectively. The biocomposite with 10 wt.% of PU1000 was characterized by the highest thermal stability. It has been observed that the increase of PU1000 content in the composite leads to an increase in the thermal stability up to the content of 10 wt.%. Moreover, a further increase of PU1000 content caused the decrease thermal parameters. The thermal stability of composites based on PU400-10 and PU400-15 was similar and comparable with that of PU1000-15.

Table 4. TG and DTG data of biocomposites based on P3HB matrix with PU400 and PU1000 addition, obtained at the heating rate of 5 deg · min<sup>-1</sup>

Sample code	$T_{on}$ [°C]	$T_{50\%}$ [°C]	$T_{max1}$ [°C]	$T_{max2}$ [°C]	$\Delta m$ [%]
P3HB	236	241	243	–	98.90
PU400-10	265	275	277	–	99.62
PU400-15	264	276	278	–	99.48
PU1000-10	270	280	281	367	99.60
PU1000-15	263	277	276	355	99.67

### 3.5. DSC analysis of biocomposites

In Figure 3a, the experimental heat flow rate is shown as a function of temperature of P3HB and PU400 biocomposites (5–20 wt. %) obtained of the second heating scan for rate of 10 °C · min<sup>-1</sup> in the temperature range between –40 °C and 195 °C prior to cooling in the same rate from temperature range of 195 °C to –40 °C.

The qualitative thermal analysis was carried out based on the heat flow rate of the semicrystalline P3HB and its biocomposites. The glass transition and the melting were observed during the heating scan for all materials. The cold crystallization was only recorded for biocomposites between the glass transition and melting region (Fig. 3). All thermal parameters of phase transitions were estimated and are listed in Table 5. The change of heat capacity at  $T_g$ ,  $\Delta C_p$ , and the glass transition temperature,  $T_g$ , were estimated

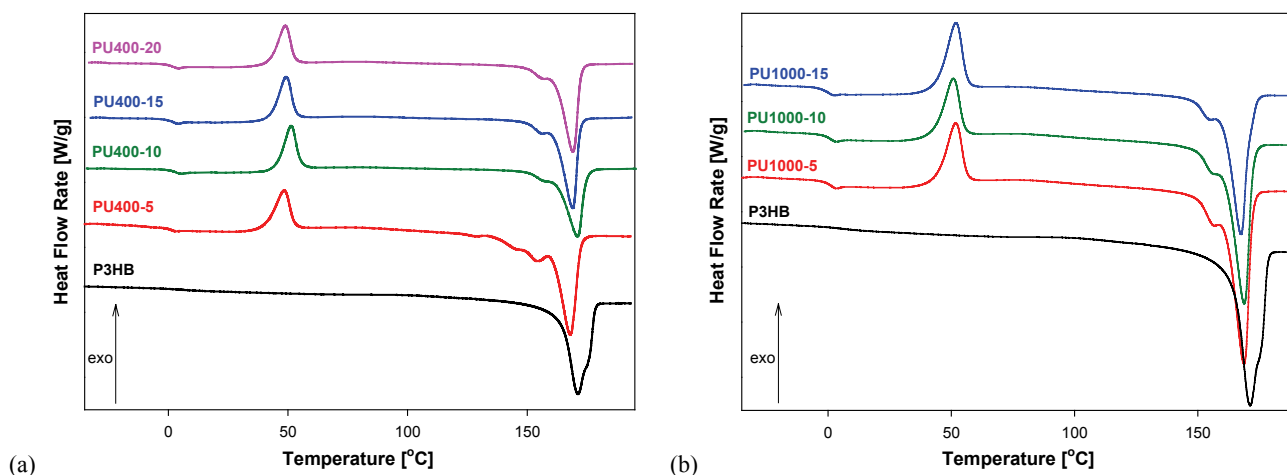


Fig. 3. Dependences of heat flow rate on temperature for: a) PU400, b) PU1000 biocomposites

 Table 5. Comparison of the thermal parameters of the P3HB composites with PU400 samples obtained with a heating at a rate of  $10\text{ }^{\circ}\text{C}\cdot\text{min}^{-1}$  after cooling at the same rate

Sample	$T_g$ [ $^{\circ}\text{C}$ ]	$\Delta C_p$ [ $\text{J}\cdot\text{g}^{-1}\cdot^{\circ}\text{C}^{-1}$ ]	$T_{m(\text{onset})}$ [ $^{\circ}\text{C}$ ]	$\Delta H_f$ [ $\text{J}\cdot\text{g}^{-1}$ ]	$T_c$ [ $^{\circ}\text{C}$ ]	$\Delta H_c$ [ $\text{J}\cdot\text{g}^{-1}$ ]
P3HB	7.70	0.48	159.7	91.93	104.80	88.79
PU400-5	-9.20	0.05	159.8	47.03	76.90	32.50
PU400-10	2.10	0.23	161.9	11.79	70.70	6.28
PU400-15	0.30	0.34	160.9	18.40	77.90	10.87
PU400-20	0.40	0.26	161.1	21.51	72.10	13.32

from the study of the glass transition region under heating. The heat of fusion,  $\Delta H_f$ , and the melting temperature,  $T_{m(\text{onset})}$ , were also estimated based on the analysis of melting region.

The heat of crystallization,  $\Delta H_c$ , and the crystallization temperature,  $T_c$ , were analyzed under the cooling process. Furthermore, the ratio  $T_m/T_g$  has been proposed as a fragility indicator [17]. The  $T_m/T_g$  was estimated to be 1.54, 1.64, 1.58, 1.59 and 1.59, respectively, for P3HB, PU400-5, PU400-10, PU400-15 and PU400-20.

The data presented in Fig. 4 are related to the constant value of heating and cooling rate of  $10\text{ }^{\circ}\text{C}\cdot\text{min}^{-1}$ . The different thermal history of biocomposites were also investigated. The dependence of the changes of heat capacity at  $T_g$  on the heat of fusion obtained from the different cooling rates are shown graphically in Figs. 4a–d. The P3HB matrix was investigated in our previous paper [6]. Here, it should be noted that changes of heat capacity and other phase transition parameters were established using the qualitative thermal analysis compared to the quantitative thermal analysis described widely in literature [6], [7]. Most of semicrystalline polymeric materials have three phases in the solid state: the crystalline phase (c), the mobile amorphous fraction (a) and the rigid amorphous fraction (RAF) [6]. For semicrystalline materials which

have only two phases: the mobile amorphous phase and the crystalline phase, the plot of the change of heat capacity at  $T_g$  versus the heat of fusion gives a linear behavior. The blue and black circles and the red stars show the experimental measurements. The continuous straight line was established from the result of fitting the experimental data between the fully amorphous,  $\Delta C_p$  (100%), and fully crystalline,  $\Delta H_f$  (100%), of P3HB, ( $\Delta H_f$  (100%)), is marked by the yellow circles. The change of heat capacity at  $T_g$  for fully amorphous PU400-5 was estimated as  $0.41\text{ J}\cdot\text{g}^{-1}\cdot^{\circ}\text{C}^{-1}$  and the heat of fusion for fully crystalline of PU400-5 as  $117.0\text{ J/g}$ . The experimental points which created the solid straight line are characteristic for two phase model. The points (red star and black circles) outside of the solid line indicate at the three-phase model. The red stars show the result of qualitative thermal analysis for PU400-5, PU400-10, PU400-15, and PU400-15, respectively from the DSC data in Figs. 4a–d. The dependence of the degree of amorphous phase,  $W_a$ , on the degree of crystallinity,  $W_c$ , of the P3HB biocomposites with PU400 are shown in Figs. 5a–d, respectively. The data presented in Figs. 4a–d were recalculated to  $W_a$  and  $W_c$  according to  $W_a = \Delta C_p / \Delta C_{p100\%}$ , and  $W_c = \Delta H_f / \Delta H_{f100\%}$ , respectively. The rigid amorphous fraction was estimated as  $W_{\text{RAF}} = 1 - W_a - W_c$  according to the reference [6]. All equilibrium pa-



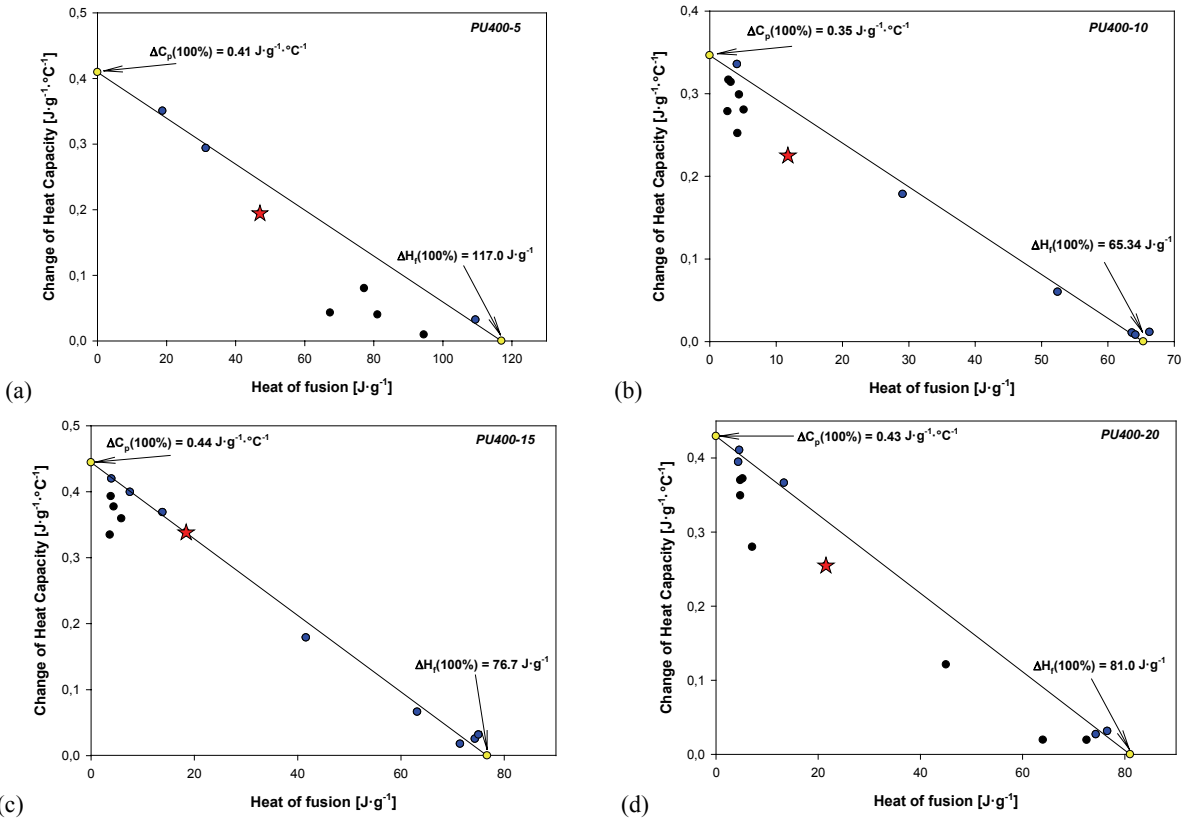


Fig. 4. The dependence of the heat capacity change at the glass transition temperature on the heat of fusion of the: a) PU400-5, b) PU400-10, c) PU400-15, d) PU400-20 composite

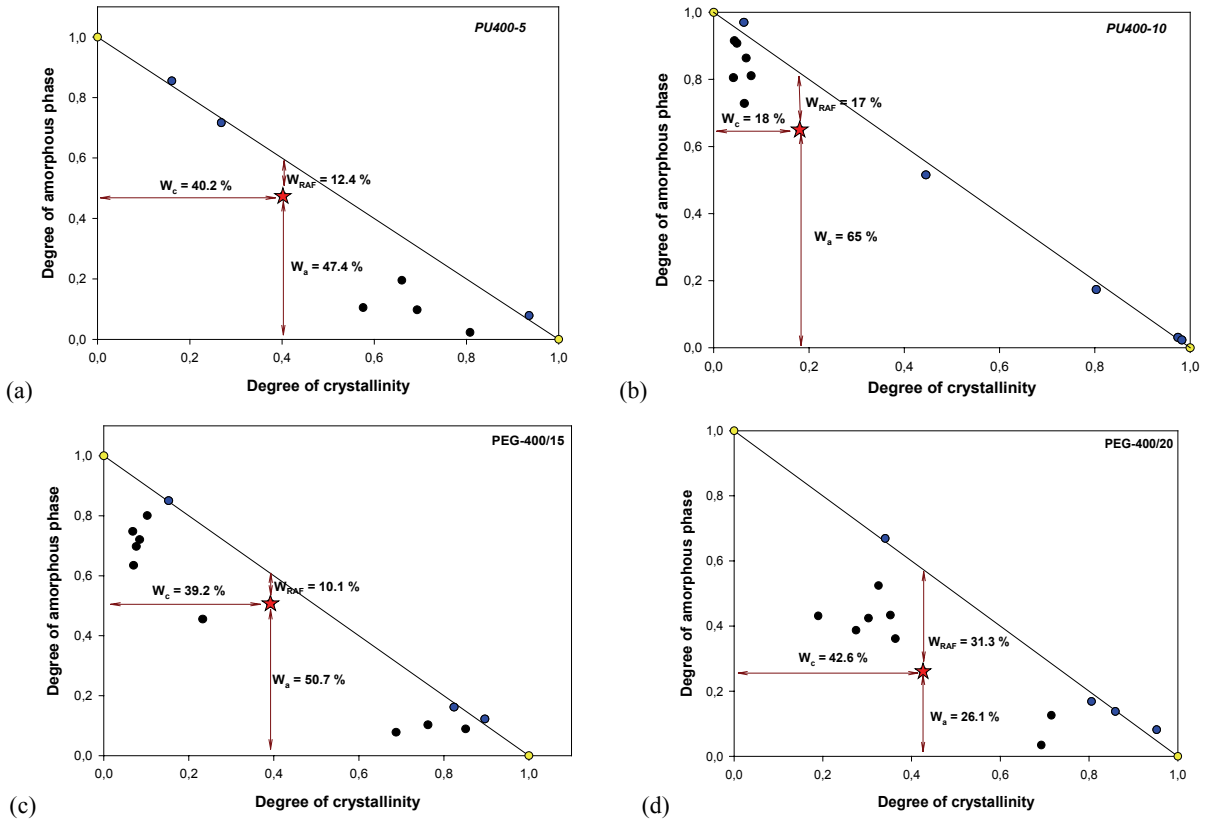


Fig. 5. The dependence of the amorphous fraction as a function of the degree of crystallinity of the semicrystalline: a) PU400-5, b) PU400-10, c) PU400-15, d) PU400-20



rameters of PU400 biocomposites were estimated and are listed in Table 6. Moreover, the set of P3HB data was collected as the reference values [23].

In Figure 3b, the dependence of heat flow rate on temperature for the PU1000 biocomposites in reference to the P3HB matrix is shown. The glass transition and melting region were observed for all analyzed material but the cold crystallization was noticed for only composites in the region between the glass transition and the melting. The qualitative thermal analysis was performed in a similar manner to the previous one. The results are collected in Table 7. The increase in melting temperature ( $T_{m(\text{onset})}$ ) was observed for the PU1000-5 and PU1000-10 biocomposites but the melting temperature of PU1000-15 was the same as that of the P3HB matrix. The crystallization temperature decreased for all biocomposites in relation to P3HB. Moreover, a plasticizing effect was observed because the glass transition temperature of biocomposites decreased compared to P3HB. The heat of fusion ( $\Delta H_f$ ) and heat capacity ( $\Delta C_p$ ) were recalculated using the equilibrium parameters and presented in Table 8 as degree of crystallinity and mobile amorphous fraction, respectively.

Furthermore, the  $T_m/T_g$  ratio has been also proposed as a fragility indicator [17]. The  $T_m/T_g$  was es-

timated using temperatures in the Kelvin scale to be 1.54, 1.59, 1.59, 1.59, respectively for P3HB, PU1000-5, PU1000-10 and PU1000-15. It can be seen that all PU1000 biocomposites have the same fragility indicator and amount of PU did not change the fragility but an addition of PU1000 caused a plasticization of new biocomposites increasing their  $T_m/T_g$  indicator in relation to the P3HB matrix.

The analysis of phase content was also carried out and its results were listed in Table 8. All analyses were carried out in a similar way as previously for PU400 (see Figs. 4a–d).

### 3.6. Spectral analysis of the P3HB biocomposites

Spectral analysis showed similar changes in the set of FTIR spectra of composites obtained with PU400 and PU1000. The FTIR spectra of the unfilled P3HB, PU1000 and biocomposites with the PU1000 addition are shown in Fig. 7. In the IR spectrum of the unfilled P3HB, a characteristic band derived from the vibrations of the ester carbonyl groups was observed at  $1717\text{ cm}^{-1}$ . Also asymmetric and symmetrical vibrations bands of C-O bonds of the ester are observed at

Table 6. Comparison of the phase content of P3HB, PU400-5, PU400-10, PU400-15 and PU400-20 representative samples obtained by heating at a rate of  $10\text{ }^\circ\text{C}\cdot\text{min}^{-1}$  after cooling at the same rate

Sample	$W_a$ [%]	$\Delta C_p$ (100%) [ $\text{J}\cdot\text{g}^{-1}\cdot^\circ\text{C}^{-1}$ ]	$W_c$ [%]	$\Delta H_f$ (100%) [ $\text{J}\cdot\text{g}^{-1}$ ]	$W_{\text{RAF}}$ [%]
P3HB	37.0	0.480	63.0	142.0	0
PU400-5	47.4	0.410	40.2	117.0	12.4
PU400-10	65.0	0.346	18.0	65.3	17.0
PU400-15	76.1	0.444	23.9	76.7	0
PU400-20	59.2	0.430	26.6	81.0	14.2

Table 7. Comparison of the thermal parameters of the P3HB composites with PU1000 samples obtained by heating at a rate of  $10\text{ }^\circ\text{C}\cdot\text{min}^{-1}$  after cooling at the same rate

Sample	$T_g$ [ $^\circ\text{C}$ ]	$\Delta C_p$ [ $\text{J}\cdot\text{g}^{-1}\cdot^\circ\text{C}^{-1}$ ]	$T_{m(\text{onset})}$ [ $^\circ\text{C}$ ]	$\Delta H_f$ [ $\text{J}\cdot\text{g}^{-1}$ ]	$T_c$ [ $^\circ\text{C}$ ]	$\Delta H_c$ [ $\text{J}\cdot\text{g}^{-1}$ ]
P3HB	7.7	0.48	159.70	91.93	104.80	88.79
PU1000-5	0.1	0.34	160.50	30.51	76.05	21.31
PU1000-10	-0.43	0.30	160.30	26.58	66.80	17.54
PU1000-15	-1.15	0.32	159.70	17.15	71.05	9.53

Table 8. Comparison of the phase content of P3HB, PU1000-5, PU1000-10, PU1000-15 and PU1000-20 samples obtained by heating at a rate of  $10\text{ }^\circ\text{C}\cdot\text{min}^{-1}$  after cooling at the same rate

Sample	$W_a$ [%]	$\Delta C_p$ (100%) [ $\text{J}\cdot\text{g}^{-1}\cdot^\circ\text{C}^{-1}$ ]	$W_c$ [%]	$\Delta H_f$ (100%) [ $\text{J}\cdot\text{g}^{-1}$ ]	$W_{\text{RAF}}$ [%]
P3HB	37.0	0.48	63.0	142.00	0
PU1000-5	71.8	0.47	28.2	106.40	0
PU1000-10	64.0	0.48	26.4	100.80	9.6
PU1000-15	76.5	0.42	19.8	86.53	3.7

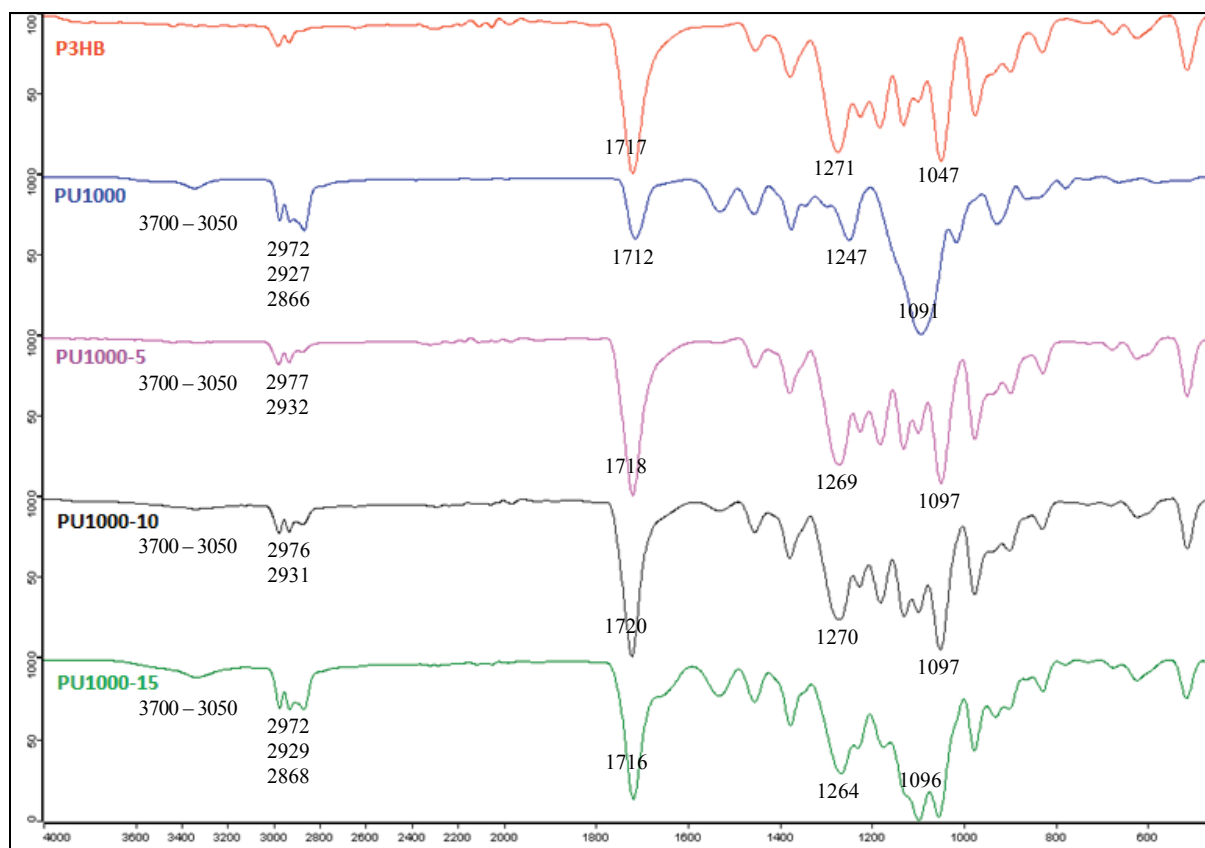


Fig. 7. FTIR spectra of P3HB, PPG1000, PU1000-5, PU1000-10, and PU1000-15

1271 as well as 1129 and 1047  $\text{cm}^{-1}$ . There were no visible bands above 3000  $\text{cm}^{-1}$ . Asymmetric and symmetric vibrations bands of the C-H bonds of the methyl and methylene P3HB groups are observed in the range of 2970 and 2920  $\text{cm}^{-1}$ .

The IR spectrum of PU1000 showed a band in the range of 3700–3050  $\text{cm}^{-1}$  derived from the valence vibrations of N-H bonds of the urethane groups. There are the distinct bands of asymmetric and symmetrical valence vibrations of the methylene and methyl groups at 2972, 2927 and 2663  $\text{cm}^{-1}$ . The valence vibrations band of urethane carbonyl groups appears at 1698  $\text{cm}^{-1}$ . The bands of symmetric and asymmetric vibrations of C-O bonds in urethane groups are observed at 1247 and 1098  $\text{cm}^{-1}$ . The band at 1098  $\text{cm}^{-1}$  overlaps with the C-O-C valence vibrations band in the structural fragment derived from glycol.

A change in the shape of the band above 3000  $\text{cm}^{-1}$  was observed in the IR spectra of the biocomposites. The band widened to the range of 3800–3000  $\text{cm}^{-1}$  due to the formation of hydrogen bonds between the urethane groups of the modifier and the P3HB ester groups. The intensity of this band increased with the increase of polyurethane content in the composite. Three bands are visible at 2977, 2930 and 2868  $\text{cm}^{-1}$  from the asymmetric and symmetrical vibrations of the

C-H bonds of the methyl and methylene groups just below 3000  $\text{cm}^{-1}$ . In the spectra of composites, there is one common vibration band of the carbonyl groups in the urethane and ester groups at 1716–1720  $\text{cm}^{-1}$ . The asymmetric vibrations band of C-O bonds of the ester and urethane appears in the range of 1270–1264  $\text{cm}^{-1}$ . Two asymmetric vibrations bands of C-O bonds are observed at 1128 and 1097  $\text{cm}^{-1}$ , similar to the FTIR spectrum of the unfilled P3HB.

### 3.7. Mechanical properties of P3HB based biocomposites

Selected mechanical properties of P3HB biocomposites containing 5, 10, 15 and 20 wt. % of PU400 and PU1000 were tested and are shown in Figs. 8 and 9. The tested biocomposites based on PU400 and PU1000 were characterized by lower tensile strength than the unfilled P3HB, as illustrated in Fig. 8a. The biocomposite containing 15 wt. % of PU1000 (PU1000-15) showed the lowest tensile strength value. The strain at break of all composites was greater than that of the unfilled P3HB (Fig. 8b). The strain at break increased by 37.5% after the introduction of polyurethane, and then did not change (PU400 composites) or oscillated

around a constant level (PU1000 composites), which was higher by 12.5% than that of the unfilled P3HB. In Figure 9b it is shown how the impact strength increased with increasing polyurethane content in the composite. Composites containing 20 wt. % of PU400 (PU400-20) were characterized by the highest impact strength (increase by approximately 90%). The impact strength of biocomposites with PU1000 also did not increase regularly with increasing polyurethane content, but the values settled at a certain level after the 30% increase. The results of the hardness are presented in Fig. 9a. The hardness of biocomposites decreased after the introduction of polyurethanes. A regular decrease in the hardness of biocomposites was observed with the increase in the content of both PU400 and PU1000.

The maximum decrease in hardness of about 60% compared to unmodified P3HB was shown by the biocomposite containing 15 wt. % of PU100, due to the plasticization of the matrix.

### 3.8. Statistical analysis

The mechanical properties of the obtained biocomposites, for which a series of measurements were performed, i.e., tensile strength, strain at break and impact strength, were subjected to statistical analysis. Its aim was to answer the question of whether the values of the analyzed mechanical properties of individual composite samples differ from the unfilled P3HB and from each other. Based on normality checked by the Shapiro–Wilk test, the significance level ( $\alpha$ ) was adopted in the tests as equal to 0.05. The tests of normality show that the values of tensile strength, strain at break and impact strength of individual composites have normal distributions. Then the *t*-test (Student’s test) was performed. From the calculated values of the *t*-test and the *p*-value it follows that:

- a) the tensile strength values are not statistically significant only for PPG-400/5 and PPG-1000/5, i.e.,

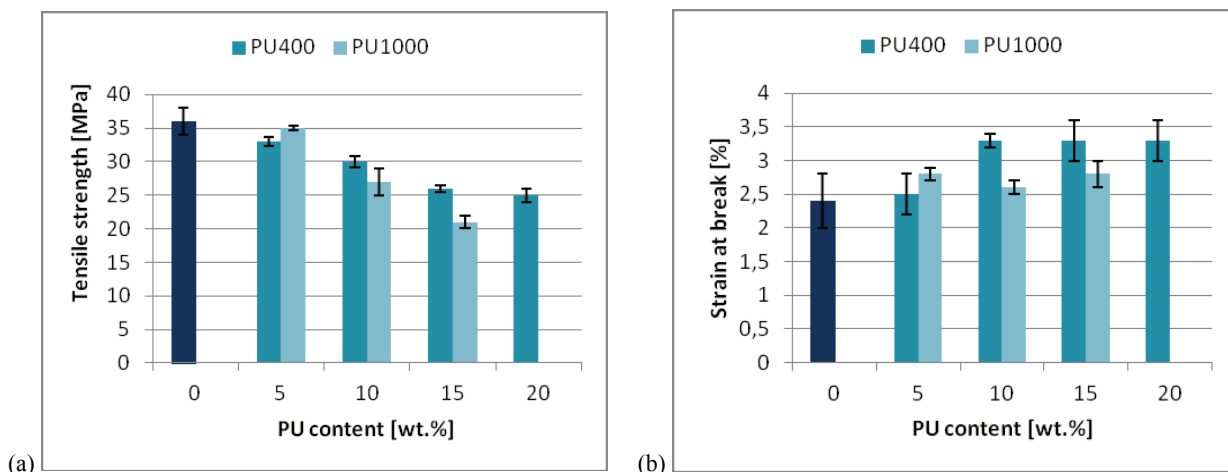


Fig. 8. Effect of PU content on the tensile strength (a) and strain at break (b) of P3HB

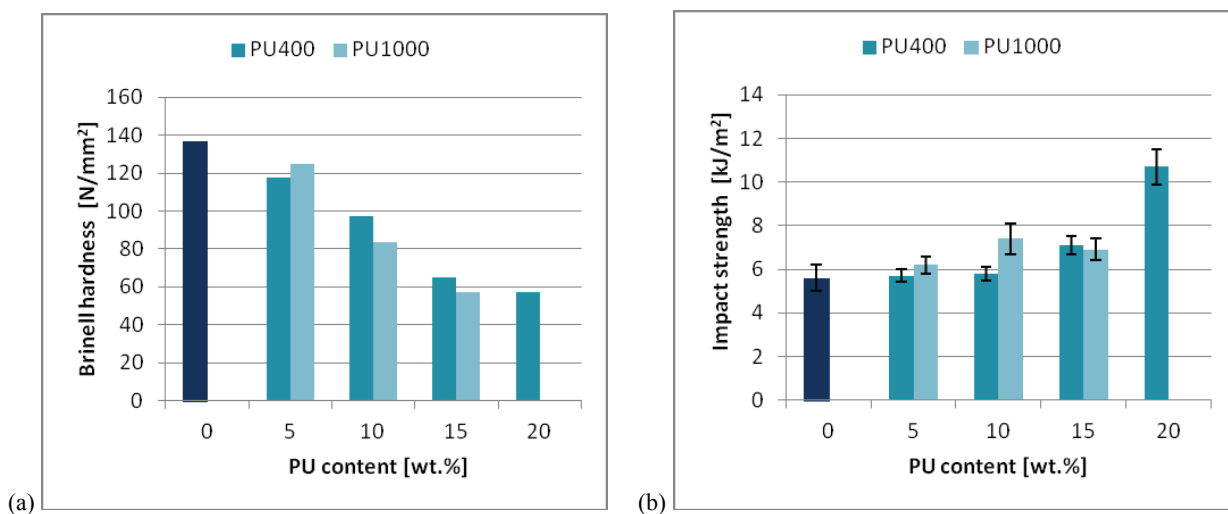


Fig. 9. Effect of PU content on the hardness (a) and impact strength (b) of P3HB

- they do not differ from P3HB, while for other composites and P3HB, they differ significantly;
- b) the strain at break values are not statistically significant only for PPG-400/5, PPG-1000/10 and PPG-1000/15, i.e., they do not differ from P3HB, while for other composites and P3HB they differ significantly,
  - c) the impact strength values are not statistically significant only for the PPG-400/5 and PPG-400/10, i.e., they do not differ from P3HB, while for other composites and P3HB they differ significantly.

Then, a one-way analysis of variance (ANOVA) was performed for the examined mechanical properties. After checking the differences between the means of the individual variables, *post-hoc* tests were performed, (Scheffe and Duncan), which made is possible: (a) to trace significant differences between the variables and (b) to observe which of the variables form homogeneous groups. The calculated value of the *F*-test (analysis of variance) and the *p*-value show that at least two composites differ in their mechanical properties.

The Scheffe test showed that:

- a) significant differences in tensile strength exist between the composites PPG-400/15, PPG-400/20, PPG-1000/10, PPG-1000/15 and other composites and P3HB. Moreover, P3HB, PPG-400/5, PPG-400/10 and PPG-1000/5 form group I; PPG-400/15, PPG-400/20 and PPG-1000/10 form group II; PPG-400/10, PPG-400/15 and PPG-1000/10 form group III (partially overlapping on group II); PPG-400/20 and PPG-1000/15 form group IV (also partially overlapping with group II),
- b) significant differences in strain at break are between PPG-400/5, PPG-400/10, PPG-400/20 and other composites and P3HB, moreover PPG-400/5, PPG-400/10, PPG-400/20, PPG-1000/5, PPG-1000/10 and PPG-400/15 form group I; P3HB, PPG-400/5, PPG-1000/5, PPG-1000/10 and PPG-1000/15 form group II (partially overlapping with group I); PPG-400/10, PPG-400/15, PPG-400/20, PPG-1000/5 and PPG-1000/10 form group III (partially overlapping on groups I and II),
- c) significant differences in impact strength exist between PPG-400/15, PPG-400/20, PPG-1000/10 and PPG-1000/15 and other composites and P3HB, moreover P3HB, PPG-400/5, PPG-400/10 and PPG-1000/5 form group I; PPG-400/15, PPG-1000/5 and PPG-1000/15 form group II (overlapping slightly with group I); PPG-400/15, PPG-1000/10 and PPG-1000/15 form group II (partial overlapping with group II); while the PPG-400/20 does not belong to any group.

Duncan's test showed that:

- a) significant differences in tensile strength do not occur only between PPG-400/5 and PPG-1000/5 but the differences are statistically significant between the other composites and P3HB. Moreover, PPG-400/15, PPG-400/20 and PPG-1000/10 form group I; P3HB, PPG-400/5 and PPG-1000/5 form group II, PEG-400/15; while PPG-400/10 and PPG-1000/15 do not belong to any group,
- b) significant differences in strain at break do not occur only between PPG-400/5 and PPG-1000/15, the differences are statistically significant between the other composites and P3HB, moreover PPG-400/5, PPG-1000/5, PPG-1000/10 and PPG-1000/15 form group I; P3HB, P3HB, PPG-400/5 and PPG-1000/15 form group II (overlapping with group I); PPG-400/10, PPG-400/15 and PPG-400/20 form group II; while PPG-1000/5 and PPG-400/20 form group IV (partial overlapping with groups I and III),
- c) significant differences in impact strength do not occur only between PPG-400/5 and PPG-400/10, the differences are statistically significant between the other composites and P3HB. Moreover, P3HB, PPG-400/5 and PPG-400/10 form group I; PPG-400/10 and PPG-1000/5 form group II (overlapping with group I); PPG-400/15, PPG-1000/15 form group III; PPG-400/15 and PPG-1000/10 (overlapping with group III); while PPG-400/20 do not belong to any group.

Ultimately, statistical tests show that there are statistically significant differences between the composites and P3HB for the three mechanical properties tested. Thus, the composites have different mechanical properties compared to the unfilled P3HB and also between them.

## 4. Discussion

Linear aliphatic polyurethanes based on polypropylene glycols (PPG) (with a molecular weight of 400 and 1000 g·mol<sup>-1</sup>) and hexamethylene diisocyanate (HDI) have been used to improve the properties of P3HB. PPG400 and PPG1000 were used to investigate the effect of the polyoxypropylene chain length (flexible segment) of polyurethane on the properties of P3HB biocomposites. The structure and surface morphology of polymer composite samples were examined using SEM. SEM micrographs of P3HB and its biocomposites containing 5, 10, 15 and 20 wt.% of PU400 and PU1000 explain the failure mechanisms that affect the mechanical properties of the tested

samples. The smallest addition, i.e., 5 wt. % of PU400, to the polyester matrix allowed the interfacial compatibility of the polymers and positively affected the reinforcement of the polyester matrix. The P3HB biocomposites containing 5 wt. % of PU400 (PU400-5), therefore exhibited the highest tensile strength. However, the composite with 5 wt. % of PU1000 contained domains which were not uniformly distributed throughout the sample and formed aggregates. The introduction of the modifier in the amount of 10 and 15 wt. % into the polyester matrix eliminated the possibility of aggregates formation. The absence of polyurethane aggregates and evenly distributed domains in the form of rough areas should determine satisfactory mechanical properties of the composites. However, the use of a solvent eliminated the aggregates in polyurethane, influencing the homogenization of the mixture before extrusion and, on the other hand, it affected the presence of undesirable pores remaining after evaporation of the solvent during the production process composites, which could deteriorate the mechanical properties of the samples. The tensile strength and the hardness decreased and the elongation at break increased along with the increase of the PU content. This could be attributed to the plasticization effect of added polyurethane.

It should be noted that slight differences were observed on the fracture surfaces of samples modified with different polyurethanes. The increase in the length of the polypropylene chain in the polyurethane modifier resulted in a slight increase in the length of the domains with wavy-like and rough areas, which correlates with a slightly higher tensile strength of the selected PPG 1000-based composites than those based on PPG 400. This is also reflected in the determined values of strain at break and hardness of the tested polyester-polyurethane composites.

It was found that the thermal properties of the tested biocomposites depend on both the content and the type of polyurethane used. The presence of PU400 and PU1000 contributed to the increase in  $T_{on}$ ,  $T_{50\%}$  and  $T_{max}$ . The biocomposite with 10 wt. % of PU1000 was characterized by the highest thermal stability, i.e., its  $T_{on}$  was by 34 °C higher than that of P3HB.

The qualitative thermal analysis was carried out based on the heat flow rate of the semicrystalline P3HB and its biocomposites with PU. The addition of PU400 from 5 to 20 wt. % caused a decrease in the crystallization temperature depending on the amount of the modifier. Moreover, based on the classification system proposed by Angell [2], [5], [24], biocomposites can be classified and plasticization process can be observed. According to the "rule of thumb" for

brittleness interpretation, the ratio of  $T_m/T_g > 1.5$  indicates a strong behavior of all investigated materials [11].

In our previous study [23], biocomposites based on linear aliphatic polyurethanes, obtained by reaction of hexamethylene diisocyanate and polyethylene glycols (PEG), were used as the modifiers of P3HB. In order to check the influence of the glycol molar weight on the properties of the composites, polyethylene glycols with molecular weights of 400 and 1000 g/mole were used. Biocomposites were also produced with 5, 10, 15 and 20 wt. % of linear polyurethanes by direct mixing using a twin-screw extruder. On this basis, the comparison of the current and previously studies is possible.

It can be noted that for PU400-5 a reduction in the glass transition temperature by about 9.9 °C is observed compared to the previous results [23] obtained for biocomposites with polyurethane based on PEG. However, the greatest level in plasticization observed by a decrease of  $T_g$ , was noticed for the biocomposites obtained from 20% of PU based on PEG as described in our previous study.

The remaining properties were less promising than for PU based on PPG, since satisfactory values of the degree of crystallinity were obtained for PU1000-5, PU400-10, PU1000-10, PU1000-15 and PU400-20, where the degree of crystallinity was reduced by 34.8, 45.0, 36.6, 43.2 and 36.4 respectively, compared to P3HB. The observed decrease in the content of the crystalline phase is related to the increase in the mobile and rigid amorphous phase associated with the greater mobility of the polymer chains, which has a decisive impact on the performance properties of the materials. On the basis of obtained results, it can be seen that the introduction of polyurethane based on PPG causes better plasticization of the obtained biocomposites compared to the P3HB matrix as well as to the previously obtained biocomposites [23] with the addition of polyurethanes based on PPG. The remaining parameters are to be evaluated based on a further analysis of mechanical properties.

It was found that the mechanical properties of the tested biocomposites depend both on the content and the type of polyurethane used. All tested biocomposites were characterized by lower tensile strength compared to unfilled P3HB. It is found that the higher the content of incorporated polyurethane, the lower the tensile strength of the biocomposites. Nevertheless, the indicated tensile strength values were still within the acceptable range (above 20 MPa) [16]. In turn, the strain at break of all biocomposites was higher than that of the unfilled P3HB, most probably



due to the flexible polypropylene chains in PU [3]. It was observed that the impact strength behaved similarly and it increased with increasing PU content. Although the hardness values exhibit an opposite trend compared to strain at break and impact strength, and decreased steadily with increasing PU content, they are nevertheless still acceptable.

## 5. Conclusions

New biopolymer composites were produced with the use of aliphatic polyurethanes obtained by reacting hexamethylene diisocyanate and polypropylene glycols with molecular weight of 400 and 1000  $\text{g} \cdot \text{mole}^{-1}$  as modifiers and P3HB as a matrix. Polyurethanes used in the amount of 5, 10, 15 and 20 wt. % improve the thermal properties of P3HB. New biocomposites show a higher degradation temperature than the unfilled P3HB. The composite containing 10 wt. % of PU1000 had the greatest difference in the degradation temperature values compared to P3HB, amounting to 34 °C. Moreover, the resulted biocomposites show higher difference in the value of the melting temperature and the degradation temperature. Usually, the difference was about 100 °C but in the case of PU1000-10 it is the highest and reaches 111 °C. It gives a wider processing window in relation to the unfilled P3HB.

The biggest changes of parameters were noted between the unfilled P3HB and biocomposites that contain 10% filler in the polymer matrix. It can be observed that values of the  $T_g$ ,  $T_c$  decreased and  $T_{m(\text{onset})}$  increased. The decrease of  $T_g$  is due to the plasticizing effect of material and is linking with the introduced modifier. Moreover, the influence of PU on the heat of fusion of semi-crystalline and fully crystalline biocomposites is also observed. This results cause a direct change of the degree of crystallinity according to  $W_c = \Delta H_f / \Delta H_{f100\%}$ . The addition of 10 wt. % of the modifier causes a 3-times decrease of  $W_c$  and the increase of amorphous content in the reference to the polymeric matrix. The prepared biocomposites were characterized by a lower glass transition temperature and degree of crystallinity compared to the unfilled P3HB. The greatest reduction in the degree of crystallinity is shown by biocomposites containing 10 and 15 wt.% of PU400 and PU1000. Additionally, the increase of amorphous phase inside the obtained biocomposite confirms that polyurethanes does not negative influence on biodegradability of poly(3-hydroxybutyrate). It can be stated with high probability that the introduction of the modifier in the

polymer matrix causes a significant enhancement of the mobility of polymer chains, and striving for a state of non-orderliness of the material. Increasing the free spaces between the polymer chains in composites increases the availability to the chains of molecules for microorganisms. Greater content of amorphous phase, better availability for microorganisms and the use of linear molecules can maintain a positive impact on the biodegradation of materials. These promising properties give hope for the use of this cheap composite in tissue engineering.

Additionally, the relationship between the topography of the material structure, and the observed thermal and mechanical properties can be noted. P3HB biocomposites with homogeneous structure confirmed by SEM showed an improvement in impact strength and strain at break. Changes of heat of fusion cause an decrease of the degree of crystallinity, which causes an decrease in strength and elasticity and the expected enhancement in the elongation value. Generally, the best properties were shown by the biocomposite obtained with 10 wt. % of polyurethane obtained from the reaction with polypropylene glycol with a molecular weight of 1000  $\text{g} \cdot \text{mole}^{-1}$  (PU1000-10).

Considering the properties of P3HB and polyurethanes, i.e., the biodegradability and biocompatibility of P3HB as well as the biocompatibility of polyurethanes, the new biocomposites offer possibilities for obtaining new products from poly(3-hydroxybutyrate) including products to medical application for tissue engineering.

## References

- [1] ALVAREZ-SANTULLANO N., VILLEGAS P., MARDONES M.S., DURÁN R.E., DONOSO R., GONZÁLEZ A., SANHUEZA C., NAVIA R., ACEVEDO F., PÉREZ-PANTOJA D., SEEGER M., *Genome-Wide Metabolic Reconstruction of the Synthesis of Polyhydroxyalkanoates from Sugars and Fatty Acids by Burkholderia Sensu Lato Species*, *Microorganisms*, 2021, 9, 1290.
- [2] ANGELL C.A., *Relaxation in liquids, polymers and plastic crystals – strong/fragile patterns and problems*, *J. Non-Cryst. Solids*, 1991, 131–133, 13–31.
- [3] ASHRAFI M., GHASEMI A.R., HAMADANIAN M., *Optimization of thermo-mechanical and antibacterial properties of epoxy/polyethylene glycol/MWCNTs nano-composites using response surface methodology and investigation thermal cycling fatigue*, *Polym. Test.*, 2019, 78, 105946.
- [4] BALART R., GARCIA-GARCIA D., FOMBUENA V., QUILES-CARRILLO L., ARRIETA M.P., *Biopolymers from Natural Resources*, *Polymers*, 2021, 13, 2532.
- [5] BÖHMER R., NGAI K.L., ANGELL C.A., PLAZEK D.J., *Nonexponential relaxations in strong and fragile glass formers*, *J. Chem. Phys.*, 1993, 99, 4201–4209.

- [6] CZERNIECKA-KUBICKA A., ZARZYKA I., PYDA M., *Advanced analysis of poly(3-hydroxybutyrate) phases based on vibrational heat capacity*, J. Therm. Anal. Calorim., 2017, 127, 905–914.
- [7] CZERNIECKA-KUBICKA A., ZIELECKI W., FRĄCZ W., JANUS-KUBIAK M., KUBISZ L., PYDA M., *Vibrational heat capacity of the linear 6,4-polyurethane*, Thermochim. Acta, 2020, 683, 178433.
- [8] D20 Committee, *Specification for Labeling of Plastics Designed to be Aerobically Composted in Municipal or Industrial Facilities*.
- [9] European Bioplastics, *Bioplastics facts and figures*. [https://docs.european-bioplastics.org/publications/EUBP\\_Facts\\_and\\_figures.pdf](https://docs.european-bioplastics.org/publications/EUBP_Facts_and_figures.pdf), Accessed: April 30, 2018.
- [10] FERRONATO N., TORRETTA V., *Waste Mismanagement in Developing Countries: A Review of Global Issues*, Int. J. Environ. Res. Public Health, 2019, 16, 1060.
- [11] KAUSHAL A., BANSAL A., *Thermodynamic behavior of glassy state of structurally related compounds*, Eur. J. Pharm. Biopharm., 2008, 69, 1067–1076.
- [12] KETTL K.-H., TITZ M., KOLLER M., SHAHZAD K., SCHNITZER H., NARODOSLAWSKY M., *Process design and evaluation of bio-based polyhydroxyalkanoates (PHA) production*, Chem. Eng. Trans., 2011, 25, 983–988.
- [13] KUMAR V., DARNAL S., KUMAR S., KUMAR S., SINGH D., *Bioprocess for co-production of polyhydroxybutyrate and violacein using Himalayan bacterium Iodobacter sp. PCH194*, Bioresour. Technol., 2021, 319, 124235.
- [14] MACHADO G., SANTOS F., LOUREGA R., MATTIA J., FARIA D., EICHLER P., AULER A., *Biopolymers from Lignocellulosic Biomass: Feedstocks, Production Processes, and Applications*, Lignocellulosic Biorefining Technol., 2020, 125–158.
- [15] MITURA S., SIONKOWSKA A., JAISWAL A., *Biopolymers for hydrogels in cosmetics: review*, J. Mater. Sci. Mater. Med., 2020, 31, 50.
- [16] PRZYBYLEK M., BIAŁKOWSKA A., BAKAR M., KOSIKOWSKA U., SZYMBORSKI T., *Effect of aging conditions on the mechanical properties and antimicrobial activity of elastomer nanocomposites*, J. Polym. Eng., 2019, 39, 316–325.
- [17] SLADE L., LEVINE H., *Glass Transitions and Water-Food Structure Interactions*, Advances in Food and Nutrition Research, 1995, 38, 103–269.
- [18] SZEWCZENKO J., KAJZER W., KAJZER A., BASIAGA M., KACZMAREK M., ANTONOWICZ M., NOWIŃSKA K., JAWORSKA J., JELONEK K., KASPERCZYK J., *Biodegradable polymer coatings on Ti6Al7Nb alloy*, Acta Bioeng. Biomech., 2019, 21, 83–92.
- [19] VOLOVA T., KISELEV E., NEMTSEV I., LUKYANENKO A., SUKOVATYI A., KUZMIN A., RYLTSOVA G., SHISHATSKAYA E., *Properties of degradable polyhydroxyalkanoates with different monomer compositions*, Int. J. Biol. Macromol., 2021, 182, 98–114.
- [20] World Health Organization, *WHO calls for more research into microplastics and a crackdown on plastic pollution*, <https://www.who.int/news/item/22-08-2019-who-calls-for-more-research-into-microplastics-and-a-crackdown-on-plastic-pollution>, Accessed: September 15, 2021.
- [21] WOŻNA A.E., JUNKA A., HOPPE V.W., *Influence of the different composites (PLA/PLLA/HA/β-TCP) contents manufactured with the use of additive laser technology on the biocompatibility*, Acta Bioeng. Biomech., 2021, 23, 169–180.
- [22] WUNDERLICH B., *Thermal analysis of polymeric materials*, Springer, Berlin 2005.
- [23] ZARZYKA I., CZERNIECKA-KUBICKA A., HEĆLIK K., DOBROWOLSKI L., PYDA M., LEŚ K., WALCZAK M., BIAŁKOWSKA A., BAKAR M., *Thermally stable biopolymer composites based on poly(3-hydroxybutyrate) modified with linear aliphatic polyurethanes – preparation and properties*, Acta Bioeng. Biomech., 2021, 23.
- [24] ZHOU D., ZHANG G.G.Z., LAW D., GRANT D.J.W., SCHMITT E.A., *Physical Stability of Amorphous Pharmaceuticals: Importance of Configurational Thermodynamic Quantities and Molecular Mobility*, J. Pharm. Sci., 2002, 91, 1863–1872.